The Functional Role of Selenocysteine (Sec) in the Catalysis Mechanism of Large Thioredoxin Reductases: Proposition of a Swapping Catalytic Triad Including a Sec-His-Glu State

Wolfgang Brandt* and Ludger A. Wessjohann[a]

*Thioredoxin reductases catalyse the reduction of thioredoxin disulfide and some other oxidised cell constituents. They are homodimeric proteins containing one FAD and accepting one NADPH per subunit as essential cofactors. Some of these reductases contain a selenocysteine at the C terminus. Based on the X-ray structure of rat thioredoxin reductase, homology models of human thioredoxin reductase were created and subsequently docked to thioredoxin to model the active complex. The formation of a new type of a catalytic triad between selenocysteine, histidine and a glutamate could be detected in the protein structure. By means of DFT (B3LYP, lacv3p**) calculations, we could show that the formation of such a triad is essential to support the proton transfer from selenol to a histidine to stabilise a selenolate anion, which is able to interact with the disulfide of thioredoxin and catalyses the reductive disulfide opening. Whereas a simple proton transfer from selenocysteine to histidine is thermodynamically disfavoured by some 18 kcal mol^{-1}, it becomes favoured when the carboxylic acid group of a glutamate stabilises the formed imidazole cation. An identical process with a cysteine instead of selenocysteine will require 4 kcal mol^{-1} more energy, which corresponds to a calculated equilibrium shift of ~1000:1 or a 10^3 rate acceleration: a value close to the experimental one of about 10^2 times. These results give new insights into the catalytic mechanism of thioredoxin reductase and, for the first time, explain the advantage of the incorporation of a selenocysteine instead of a cysteine residue in a protein.*

Introduction

Thioredoxin reductases (TrxR) catalyse the NADPH-dependent reduction of a disulfide bridge in oxidised thioredoxin (Trx). They are present in bacteria, yeast, animals and plants.[1,2] In particular, mammalian TrxRs show an unusually broad substrate specificity as they also accept nondisulfide substrates such as vitamin K,[1] alloxan,[3] sodium selenite, selenocystines,[4] S-nitrosoglutathione and arachidonic acid hydroperoxides.[5] TrxRs are homodimeric proteins containing one flavin adenine dinucleotide (FAD) and accepting one NADPH per subunit as essential cofactors. Recently it was revealed that thioredoxin reductases from *Plasmodium falciparum* and humans represent a novel class of enzymes, called large thioredoxin reductases. Interestingly, some of these contain a selenocysteine (Sec: one letter code U) at the C terminus. It has been shown that selenocysteine plays an important role in the catalytic mechanism. Its removal by carboxypeptidase digestion[6] or its modification by alkylation[6,7] leads to complete inactivation of the enzyme. Furthermore, selenium deficiency causes a considerable loss of TrxR activity.[8–12] When Sec498 of hTrxR (human TrxR) was replaced by Cys, a 100-fold lower k_{cat} for the reduction of Trx resulted.[13] Since many TrxRs have an unusually broad substrate specificity,[1,4,5,14] they are involved in a multitude of metabolic pathways and play a crucial role in many diseases, such as rheumatoid arthritis,[15–17] and AIDS.[18–20] An excellent overview about aspects of pathological factors and TrxRs as drug targets is given by Becker et al.[21] For example, based on the special role of selenocysteine in human TrxR, the gold-containing drug auranofin has been found to be active against rheumatic problems.[16,22,23]

Knowledge of the 3D structure of human TrxR and a detailed understanding of its catalytic mechanism, especially of the role of selenocysteine therein, might considerably enhance the possibility of developing specific inhibitors and improved or new drugs against several diseases.[21]

The general catalysis mechanism accepted by most researchers is schematically represented in Scheme 1. It starts from the passage of hydride ions from NADPH to FAD (a), which are subsequently transferred to the active-site disulfide—in the case of the cytoplasmic human thioredoxin reductase the disulfide bridging Cys59 and Cys64 (b). Finally, the C-terminal Cys497 and Sec498 selenenyl–sulfide bond is reduced to form selenocysteine and cysteine (c), which than serve as a hydrogen donor to reduce the ligand's disulfide bond (d).

If there is no substrate, a thiolate-flavin complex is formed. It is quite obvious that Sec498 plays an important role in the catalysis.[6,8–13] Therefore, it is supposed that the oxidised selenocysteine–cysteine (Cys497–Sec498) takes part in the catalysis by accepting the electrons (and protons) from the active-site

[a] *Priv.-Doz. Dr. W. Brandt, Prof. Dr. L. A. Wessjohann*
Leibniz Institute of Plant Biochemistry
Department of Bioorganic Chemistry
Weinberg 3, 06120 Halle/Saale (Germany)
Fax: (+49) 345-5582-1309
E-mail: wbrandt@ipb-halle.de

  DOI: 10.1002/cbic.200400276

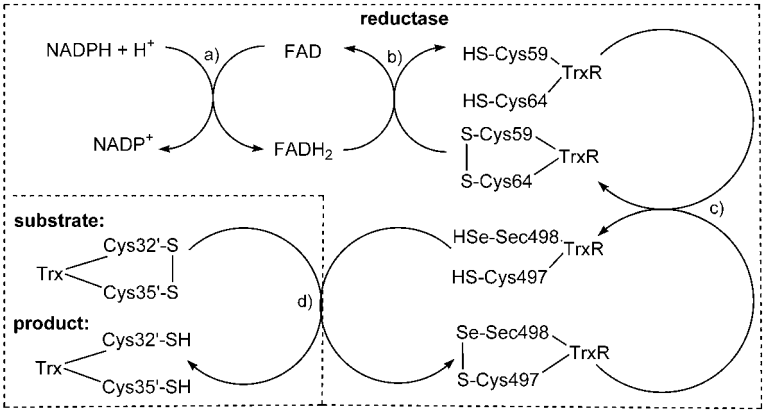

Scheme 1. *General mechanism of the action of thioredoxin reductase to reduce the substrate thioredoxin. In steps a) and b), hydride ions are transferred from NADPH + H^+ via FAD(H_2) to reduce a disulfide bond (Cys59–Cys64) of the reductase. In step c), two electrons are transferred to the C terminus of the other monomer of the dimeric protein to reduce a selenenylsulfide bridge (Cys487–Sec498). This reduced form represents the catalytically active unit to finally reduce by electron transfer the disulfide bond (Cys32′–Cys35′) of the substrate thioredoxin or other electron acceptors.*

Cys59 and Cys64. Thus Cys497 and Sec498 represent the actual reduction equivalents to reduce the substrates, for example, thioredoxin.[24,25] Furthermore, it has been shown that His509 of thioredoxin reductase from *Plasmodium falciparum* takes part in the catalysis. When this histidine was mutated to glutamine, a 95% loss of reductase activity resulted.[26] This strongly suggests that this histidine is important for the catalysis. However, it is still not known in detail how these last steps in the catalytic mechanism proceed, based on molecular structures, intermediates and transition states. An X-ray structure is available for rat thioredoxin reductase, which was solved by using a U498C mutant, but so far none has been reported for the human analogue. Moreover, no complete structure of a complex between thioredoxin reductase and thioredoxin as substrate has been reported, although an X-ray of the product Trx (reduced substrate) is available.[27]

Based on homology modelling techniques, we have developed models, first of the dimeric human thioredoxin reductase and subsequently of a complex with its substrate thioredoxin. By means of ab initio, quantum-mechanical, DFT calculations, the role of a histidine and a glutamate side chain, which to us appeared to be of high importance for effective catalysis, was studied in detail to give better insights into the catalysis mechanism and the special functional role of selenocysteine in contrast to cysteine.

Results

Based on the X-ray structure of rat thioredoxin reductase (pdb entry 1h6v),[5,6,13,28] homology models of the cytoplasmic human thioredoxin reductase (TrxR1; swiss-prot entry Q16881 as Txn1)[29] and of mitochondrial human thioredoxin reductase (TrxR2; swiss-prot entry Q9NNW7 as Txn2)[30–32] were developed. The sequence of Txn1 in the swiss-prot does not contain the important Sec498 (or Gly499), probably because the codon TGA was erroneously interpreted as stop codon.[33–35] Both residues were added to our model because they have been identified as essential parts of the protein.[31,36] The sequence identities between the templates and the target structure are 69%. This rather high identity guaranties that the models formed will represent reasonable structures very close to an experimental one. This expectation was confirmed by a PROCHECK analyses, which showed that 78.2% (and for Txn2 80.8%) of the residues were located in the most favoured region, 21.0% (18.4%) in additional and 0.8% (0.9%) in generously allowed regions of a Ramachandran Plot.[37] All other criteria for a reasonable structure, such as planarity of the peptide bonds, no bad contacts, H-bond energies and reasonable side-chain conformations, are inside or even better than in an experimental structure with an *R* value of 2.0 Å. Furthermore, comparison of plots obtained from a PROSA II analysis give nearly the same graphs in negative energy areas.[38]

Comparison of positions of the backbone atoms of the 3D structures of the modelled enzymes with those of the experimentally solved structure of rat thioredoxin reductase showed an almost identical structure. As a consequence, all discussions and considerations concerning the modelled human thioredoxin reductases can be expected to be true also for the rat one. The only major deviation between the X-ray structure and the models was detected at the C-terminal tail when the substrate thioredoxin is docked (see below).

The quality of both models has been accepted by the Protein Data Bank[39] and they have received the entry codes 1w1c (for TrxR1) and 1w1e (for TrxR2). (They can be downloaded from http://www.rcsb.org/pdb/ for a detailed inspection.) In the following discussion, for conciseness and clarity in reading, only the structure of the cytoplasmic human thioredoxin reductase (TrxR1) will be discussed, although all results can be adequately transferred to the corresponding structure of TrxR2 and to the rat thioredoxin reductase.

In the X-ray structure of dimeric rat thioredoxin reductase, the C terminus with the catalytically important cysteine residues is not close to the redox cascade with the NADPH and FAD binding sites and the active disulfide (Cys51–Cys56). By means of molecular-dynamics simulations, a stable conformation could be derived, wherein the selenocysteine is not only close to the mentioned redox cascade, but is also placed ideally to aid the putative catalytic mechanism discussed below, that is, near to His472. This histidine structurally corresponds to His509 of thioredoxin reductase from *Plasmodium falciparum*, the mutation of which to glutamine resulted in 95% loss of reductase activity.[26] This clearly shows the importance of this histidine residue and that it very likely has an essential function in the catalysis.

Figure 1 shows the secondary structure of the modelled human TrxR1. The only major deviations from the rat template protein occur at the C-terminal tails due to the applied molecular-dynamics simulation (compare the magenta-coloured backbone of the C-terminal tails of the rat enzyme in Figure 1).

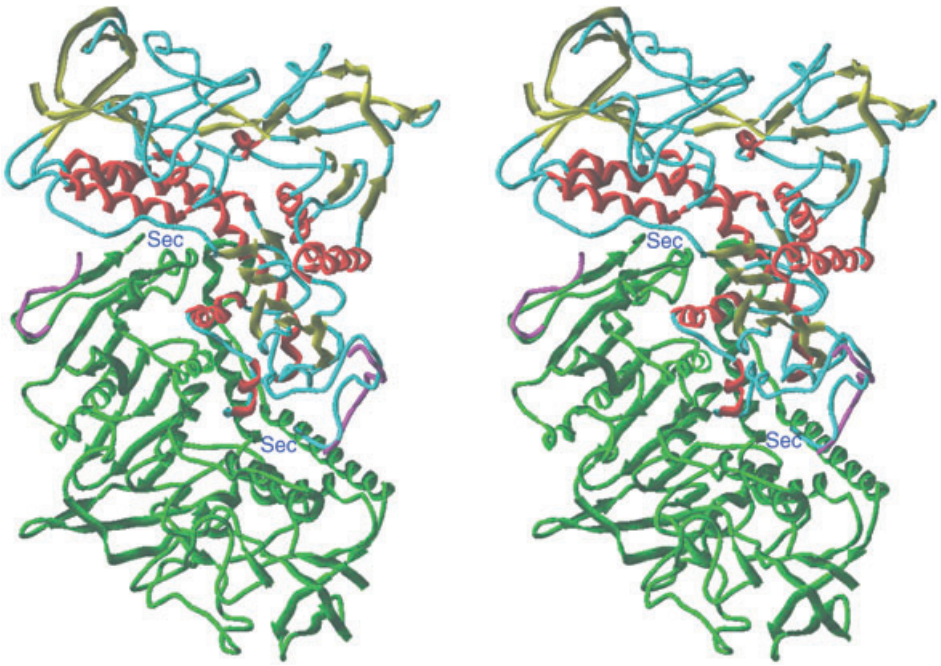

Figure 1. *Stereo representation of the secondary structure of homodimeric human thioredoxin reductase. For better clarity one monomer is colour coded for secondary structure elements (red: helices, yellow: β-sheets) and the other one is uniformly green. The magenta segments show the conformation of the C-terminal tail of the template protein of rat thioredoxin reductase for comparison.*

In the model structure, the C terminus points deeper into the cleft between the two monomers, at the bottom of which are located the active disulfide and FAD. This structure is stabilised by forming a salt bridge between the carboxyl group of the C-terminal Gly499 with the side chain of Arg351. This salt bridge is ideal for stabilising the "correct" orientation of the C terminus for it to become catalytically active.

To obtain an idea of the arrangement of thioredoxin reductase and thioredoxin as ligand to be reduced, a model of this complex was developed based on the model of human thioredoxin reductase and the X-ray structure of human thioredoxin (pdb entry 1aiu).[27] Within the substrate's X-ray structure, Asp60′ has been mutated to Asn60′. In the model we used the wild-type instead, that is, Asn60′ was modified back to Asp60′. (The prime designates an amino acid residue in the substrate.) As described in the Experimental Section, molecular-dynamics simulations were applied to analyse docking arrangements of thioredoxin to thioredoxin reductase by using a small constraint between the selenocysteine of the enzyme and the cystine of thioredoxin. The resulting complex structure is shown in Figure 2. A PROCHECK analyses of this complex showed 79.8% (for TrxR2 79.9%) of residues in the most favoured, 19.1% (18.9%) in the additionally allowed and 1.1% (1.2%) in the generously allowed regions of a Ramachandran plot. All other criteria for a reasonable structure, such as planarity of the peptide bonds, no bad contacts, H-bond energies, and reasonable side-chain conformation are inside or even better than an experimental structure with an *R* value of 2.0 Å.

In thioredoxin, during docking to the reductase, only a small change in the arrangement of the secondary-structure elements occurs, but a very close approximation of its disulfide bond to the active site of thioredoxin reductase results. The detailed structural model of the active site is shown in Figure 3. The interaction between thioredoxin and thioredoxin reductase is further stabilised by hydrophobic interactions and hydrogen bonds, but is particularly directed by the formation of strong electrostatic interactions between the side chains of Glu6′ with Lys37 and Lys124 of TrxR1, and of Lys36′ with Glu122, and of both Asp58′ and Glu56′ with Lys124. Details of this arrangement are not shown in the Figure, but can be inspected by downloading the structures stored in the protein database (1w1c and 1w1e).

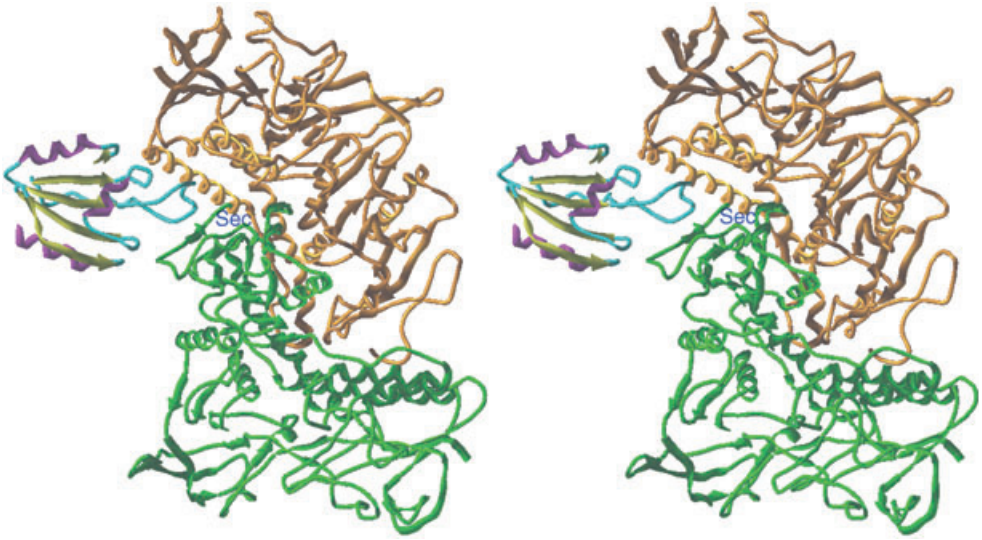

Figure 2. *Stereo representation of the secondary structure of homodimeric human thioredoxin reductase (orange and green) in complex with thioredoxin (left, colour coded for secondary structural elements).*

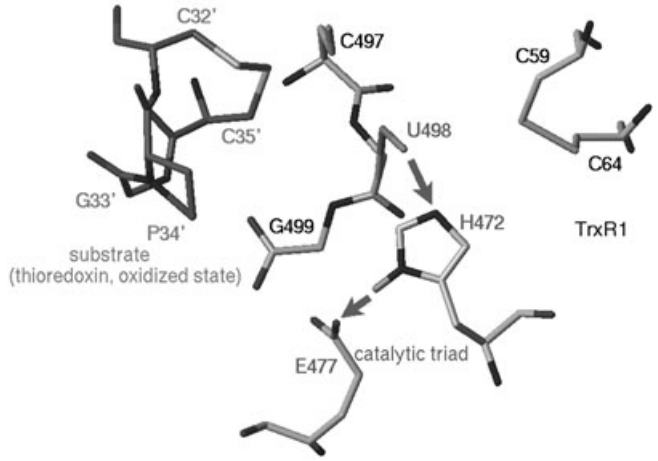

Figure 3. *The catalytically active site of thioredoxin reductase in complex with the substrate thioredoxin. The arrows indicate the proton transfer from Sec498 to His472 to form the catalytic triad together with Glu477.*

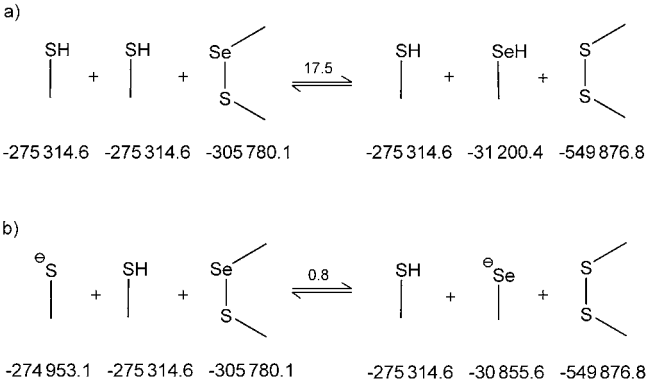

Scheme 2. *Calculations of the thermodynamic equilibrium between selenenylsulfide and disulfide a) in the case of neutral reacting groups and b) under participation of an anionic charge. Energy values under the compounds represent the total energies of the isolated compound in the gas phase in kcal mol^{-1} as obtained from DFT calculations. The resulting reaction energies (Δ_rH) for the forward reactions are given above the arrows.*

It is evident that in such an arrangement of the reactive groups (the Sec498 and Cys497 of the reductase, and Cys32′ and Cys35′ of the ligand), a catalytic hydride transfer may occur. If one has a closer look into this structure, not only are the cysteines or selenocysteines able to interact with each other, but the formation of a catalytic triad similar to those established for serine proteases[40–43] can be identified. In this special case, the catalytic triad consists of Sec498, His472 and Glu477, as labelled in Figure 3 by arrows. The critical role of histidine for the activity of thioredoxin reductases has already been discussed and demonstrated.[26] Our model shows that its function is that of a base to accept a proton from Sec498 and to form or stabilise a selenocysteine anion, which might serve as electron delivery unit to reduce the oxidised form of thioredoxin. Glutamate aids this process considerably through a relay mechanism, detaching the proton at the other imidazole nitrogen of His472. It is not yet completely understood why a selenocysteine is inserted in several thioredoxin reductases instead of a cysteine or how the catalysis proceeds in detail. On the basis of the arrangement of the reacting residues suggested here in the complex with thioredoxin, a detailed catalysis mechanism including the functional role of selenocysteine and glutamate can be studied by means of quantum-mechanical DFT calculations, and can be compared to a cysteine model analogue.

During the redox processes exhibited by the thioredoxin reductase, selenocysteine–cysteine is both reduced and oxidised by cyst(e)ines (cf. Scheme 1). If the thermodynamic equilibrium of such a process is considered (Scheme 2a), it becomes evident from the ab initio DFT calculations that the formation of the disulfide bond is about 17 kcal mol^{-1} disfavoured in comparison to a selenenyl–sulfide bond. That is, the oxidation to form the Se–S bond is feasible (Scheme 1d), but the reverse reaction (Scheme 1c) is not. Obviously, there must be a mechanism to allow the facile reduction of selenenylsulfide by dithiol to form active selenol/thiol. From the calculations presented in Scheme 2b, it becomes clear that the electron-pair transfer between the reacting groups can only proceed well when an intermediate anion (thiolate or selenolate) is formed. The corresponding thermodynamic equilibrium with incorporation of an anion instead of a protonated neutral species (Scheme 2b) now shows only a very small preference (0.8 kcal mol^{-1}) for the formation of a selenenylsulfide bond. This theoretically offers the chance to perform redox steps back and forth without high energy efforts. Thus the following questions have to be answered if one wishes to understand the whole catalytic mechanism performed by the reductase. First, how can the intermediate anions, either thiolate or selenolate, be formed in a thermodynamically favourable way; second, what is the driving force to give the product and to force the catalysis in one favoured direction, namely the reduction of the substrate; and third, what are the consequences for the transition states, that is, the speed of catalysis; finally, fourth, what is the importance and advantage of the incorporation of selenocysteine rather than cysteine in the protein?

To answer the first question, a closer consideration of our proposed new catalytic triad is crucial, that is, the roles of histidine and—newly proposed—glutamate in the chalcogenide anion formation have to be studied in detail.

In Scheme 3a and c, the results of the calculation of the thermodynamic equilibrium of a proton transfer from a methylthiol (as model for cysteine) or a methylselenol (selenocysteine) to a methylimidazole (histidine) are displayed. In both cases, the proton transfer to histidine is disfavoured by more than 18 kcal mol^{-1} (Scheme 3a and c); this would make such a process very unlikely. However, if a catalytic triad or a charge-relay system is made accessible by inclusion of the conserved Glu477, as detected in our protein models (and which is also amenable for the experimental structure of rat thioredoxin reductase), a proton transfer to histidine becomes favourable (Scheme 3b and d).

Two important conclusions can be drawn from these calculations. Thermodynamic reasons support the hypothesis that the formation of a charge-relay system consisting of a (seleno)cys-

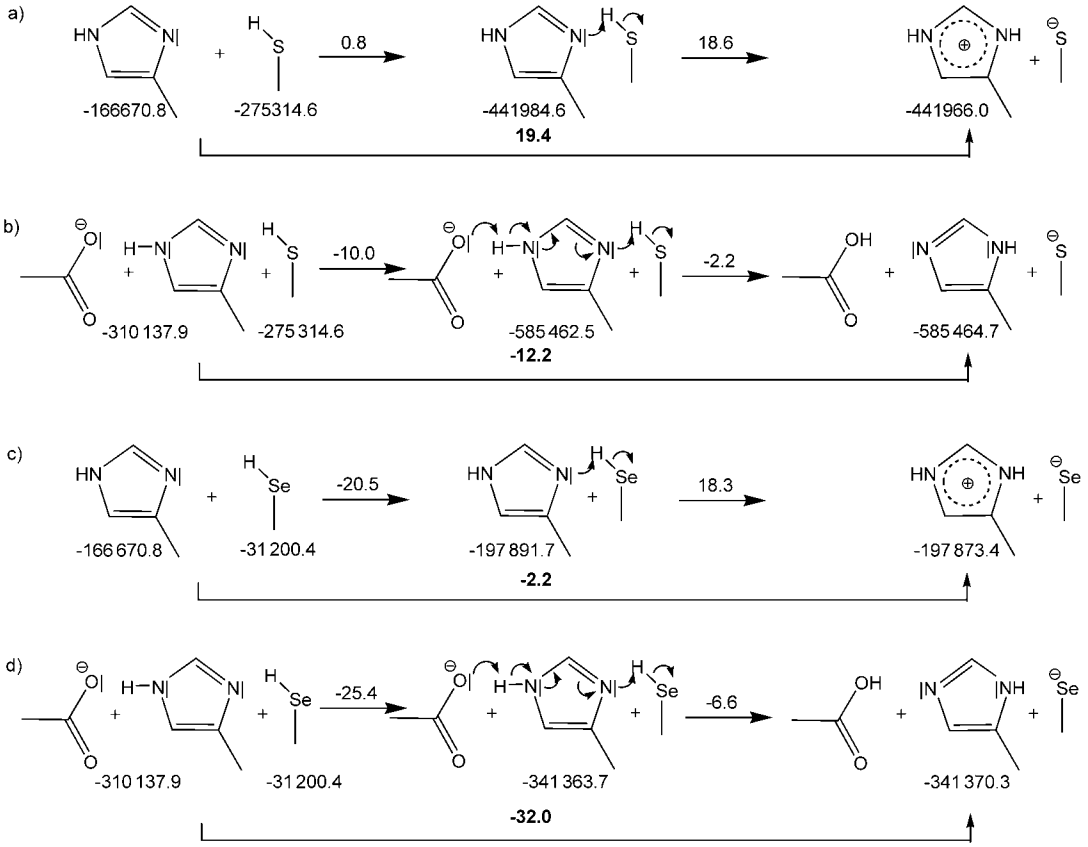

Scheme 3. *Thermodynamics of the proton transfer from selenol or thiol to imidazole without [a) or c)] and with [b) or d)] the involvement of glutamate in the form of a catalytic triad for comparison. Data are given for thiol [a),b)] and selenol [c), d)] deprotonation. Energies below the structure drawings are the sum of the energies of the isolated compounds or complexes in kcal mol^{-1} obtained from ab initio DFT calculations, whereby the first step in each reaction represents the formation of the complexes through a hydrogen bonding network and the last step represents the proton transfers. Values above the arrows show the resulting reaction energies.*

teine, a histidine and a glutamate is essential for the catalysis. Second, if the resulting energy gains in the formation of the thiolate or selenolate anion within the triad are compared, it is evident that it is much more favoured for selenol (-6.6 kcal mol^{-1}) in comparison to thiol (-2.2 kcal mol^{-1}). This result itself is not so surprising when comparing the experimental pK_a values of thiol (p$K_a = 8.3$) and selenol (p$K_a = 5.2$) with each other.[44] In the context of the formation of a catalytic triad and the role of selenocysteine in thioredoxin reductase, it has the consequence that the whole catalytic process is significantly improved, at least thermodynamically.

This becomes evident if we consider the thermodynamics of the reduction of the disulfide bond of thioredoxin under participation of the catalytic triad, which is summarised in Scheme 4. Coming to the second question to be answered: What are the driving forces in the catalysis? In the first step of the mechanism (a), the enzyme is activated by hydride transfers from NADPH via FAD to the cystine (Cys59–Cys64) to form the active, reduced cysteine intermediates of the enzyme. This mechanism is well established and accepted.

After reduction, one of these cysteines is involved in the formation of the first state of the swapping catalytic triad for deprotonation (Scheme 4 b→c) with an energy gain of -10 kcal mol^{-1}. By this, the proton can be abstracted in a thermodynamically favoured way by His472 (Scheme 4 c→d, cf. also Scheme 3 b) with an additional energy gain of -2.2 kcal mol^{-1}. The thus-formed thiolate anion is able to attack and reduce the selenenylsulfide bond of Cys497–Sec498. Accompanied by an electron-pair transfer, swapping of the catalytic triad from Cys59–His472–Glu477 to the second state Sec498–His472–Glu477 occurs. This step is thermodynamically favoured by -2.3 kcal mol^{-1} due to the higher energy gain in the formation of the catalytic triad with selenolate rather than thiolate (cf. Scheme 3 c and Scheme 4 d→e). With this step, a very active selenolate is formed that is able to reduce a substrate attached to the enzyme. The whole mechanism up to this step is thermodynamically favoured by -14.5 kcal mol^{-1} in total, and is energetically downhill.

If the selenocysteine at position 498 were a cysteine, the last step would deliver no energy gain. Therefore the activation would not proceed or at least it would be much slower (ca. 100-fold, which corresponds well to 2.3 kcal mol^{-1}); this has been experimentally proven.[13] With this result, the significance of selenocysteine in thioreductase becomes evident (cf. fourth question). Within Scheme 4, the overall reaction is the redox-interchange of the dithiol of the enzyme (cystines 59/64) with that of the substrate (cystines 32′/35′). Formally this does not change the energy content of the system under consideration.

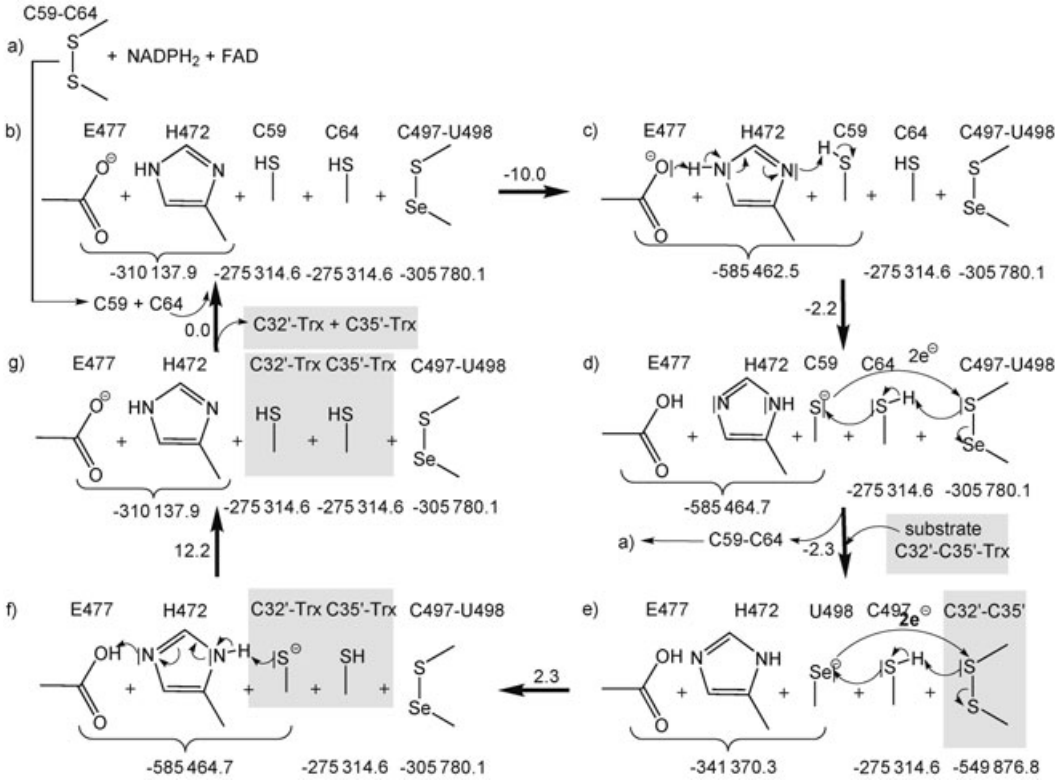

Scheme 4. *Calculation of the thermodynamics of the final two steps in the likely catalysis mechanism of large thioredoxin reductases supported by the formation of a catalytic triad with selenol. Amino acid labels correspond to those of the models shown in Figure 3. Residues highlighted with a grey background refer to the substrate thioredoxin. Energies are given in kcal mol^{-1} and represent the total energy from the DFT ab initio calculations or, next to arrows, the resulting reaction energies.*

Due to the high reactivity of the selenolate, the disulfide bond of the substrate can be reduced efficiently (Scheme 4 e→f→g, cf. Scheme 2). This process is principally identical to the reversed steps, that is, the formation of the selenolate, and consequently also needs some 14.5 kcal mol^{-1}. However, there are two major differences between the activation of the enzyme and the reduction of the substrate:

1) After the substrates disulfide bridge Cys32′—Cys35′ has been reduced, it will dissociate from the enzyme; this is accompanied by an increase of entropy from the higher flexibility of the reduced cysteines and the new degrees of freedom for translation and rotation of and especially within the free ligand.
2) A specific situation in the sequence of thioredoxin that might additionally contribute to an energy gain is the release of ring strain by reduction of the substrate. The ring of the oxidised form of thioredoxin consists of the sequence Cys32′-Gly33′-Pro34′-Cys35′, that is, it contains a [10.2.0] bicyclic ring system (proline and disulfide), which might cause ring strain that will be released by the reduction of the disulfide bond and therefore might deliver additional energy.

This hypothesis is strongly supported by the high conservation of either the Cys-Gly-Pro-Cys motif in almost all thioredoxins known (about 95%) or the even more proline-rich tricyclic sequence Cys-Pro-Pro-Cys in the rest. By using the semiempirical PM5-method, starting with the geometry from the X-ray structure of thioredoxin (open, reduced form) and of the oxidised structure used in the model complex, both tetrapeptides were optimised (causing nearly no conformational changes). The calculated heats of formation showed that the energy content of the reduced, open form is some 8.6 kcal mol^{-1} lower than that of the disulfide-bridged oxidised structure. Formally, in this reaction, a hydrogen molecule is formed of which the heat of formation is, by definition, zero. The energy difference gives an estimation of the ring strain, which will be released during the reduction process and which therefore contributes to the driving force in the overall catalysis.

Looking at the same mechanism with purely cysteine intermediates, that is, a cysteine instead of a selenocysteine, the only major difference in the thermodynamics would be the reduction of the cystine (C497—C498) and of the substrate. For both steps, the formal reaction energy again would be zero. In other words, there would be no energy gain to reduce the second disulfide bond of the enzyme to drive the redox-cascade of TrxR1 downhill and render the terminal C497—C498 active site catalytically active.

The thermodynamically favoured formation of the catalytically active selenolate in comparison to a thiolate allows not only the conclusion that the selenolate form is more likely to occur and thus more abundant, but that, as a consequence,

reduction will also proceed faster (to answer question 3). The downhill redox cascade within TrxRs will not only produce more reduced active form in the active-site cleft but will also result in increased rates. It is known from basic physical chemistry (Curtin–Hammett principle as a basis for many QSAR methods) that the transition-state energy parallels the reaction energy and that consequently the reaction should be faster. In addition, the selenolate as a "soft" semi-metal-like anion will be much more prone to polarising its electron shell and transferring electrons to the substrate faster.

Discussion

The overall model of the human thioredoxin reductases and its complex with thioredoxin is supported by the high identity score, the quality of the Ramachandran plot and the very small structural deviations from the X-ray structures of both the template rat thioredoxin reductase and thioredoxin. Nevertheless, the possibility that some details of the structure of the loop of thioredoxin that directly interacts with thioredoxin reductase may adopt a different arrangement or orientation or even cause a major structural alteration in the enzyme cannot be excluded. This uncertainty, however, will not influence the fundamental conclusions derived from the ab initio quantum-mechanical calculations, since only the thermodynamics of the reduction of the disulfide bridge occurring in thioredoxin have been considered. Direct kinetic investigations would require knowledge of the exact spatial positions of the reacting groups, which is not available.

These quantum-mechanical calculations clearly show the importance and function of a selenocysteine in the catalysis exhibited by thioredoxin reductases, which originate in the higher softness and acidity of selenocysteine ($pK_a = 5.3$) in comparison to cysteine ($pK_a = 8.3$) and lead to a much more pronounced energy gain during the reduction of the TrxR's internal disulfide bond.

The formation of a swapping (Cys-His-Glu to Sec-His-Glu) catalytic triad postulated here is very likely. First of all, the essential functional role of His472 has already been proven experimentally by site-directed mutagenesis. Furthermore, if all enzymes[34] belonging to the gene family HBG004959 are aligned, glutamate (E477) involved in the catalytic triad is 100% conserved. Even in the X-ray structure of the template protein, the rat thioredoxin reductase, this triad is preformed, and shows the interaction between the corresponding histidine and glutamate.

Furthermore, it has been shown by site-directed mutagenesis that a mutation of Gly33′ to lysine in thioredoxin leads to an approximately 2.8-fold-reduced catalytic efficiency in comparison to the wild-type.[45] This mutation mainly has an effect on K_M, that on k_{cat} being negligible. Based on the modelled structure of the complex between thioredoxin reductase and thioredoxin, this result is simple to explain and understand. On one hand, the binding pocket is so narrow that the introduction of the relatively large lysine instead of glycine leads to steric hindrances for optimal docking, on the other hand the new lysine side chain (probably even positively charged), would point directly to the side chain of Lys29 of the enzyme; this would probably cause repulsion and therefore prevent optimal docking. This finding although not conclusive by itself, additionally supports the principal correctness of the modelled structures.

Another interesting result concerning C-terminal modifications of thioredoxin reductases was found by Gromer et al.[46] These authors could show that the corresponding enzyme from *Drosophila melanogaster*, which has a Ser-Cys-Cys-Ser-COOH sequence motif at the C-terminal tetrapeptide moiety instead of the Gly-Cys-Sec-Gly-COOH found in mammalian thioredoxin reductases, is similar in enzymatic activity to the mammalian enzyme. By site-directed mutagenesis, they could further show that SCCG and GCCS-mutants improve the catalytic activity in comparison to a GCCG variant, whereas all mutants with aspartates flanking the cysteine residues had significantly lower k_{cat} values. All these experimental finding may be explained by our model of the complex between thioredoxin reductase and thioredoxin as substrate. In principal, the serine OH should be able to stabilise a thiolate, and thus render it similar in reactivity to a selenolate. A neighbouring glycine will not have that effect, and a neighbouring acid will hamper deprotonation. However, secondary effects of the altered amino acids will also have to be considered.

In the case of serine residues flanking the cysteine residues, one serine (the last) is able to form a hydrogen bond with the side chain of Gln494, and the other with His108 or with Thr412. In both cases, these interactions stabilise the active conformation of the C-terminal tetrapeptide and allow a close contact to the disulfide bond of the substrate. In contrast to this, negatively charged aspartic acid residues can give a conformational change resulting in less reactivity, either by competitive interaction of the C-terminal carboxyl group and the charged side chain of introduced Asp with Arg351 or more directly due to electrostatic repulsion by changing the conformation of the catalytically active Glu477 and thus disturbing the catalytic triad. The exact nature of the effect of neighbouring groups on Cys will have to be studied by detailed calculations in future work.

Independent of computational verification, the experimental findings of Gromer et al. indirectly also support the model of the complex between thioredoxin reductase and thioredoxin. To prove the postulated existence of a catalytic triad, point mutations, especially of Glu477 will be the subject of a future collaboration with a genetic group.

Last, but not least, the DFT calculations strongly support the catalytic function of the glutamate because, without this, the formation of a thiolate (Scheme 3a) and a selenolate therefrom (Scheme 2a) as essential steps for an electron transfer are thermodynamically highly unfavourable.

In summary, our proposed swapping triad Cys/Sec-His-Glu and especially the involvement of a selenium anion as internal redox-cascade end point drives the reduction equilibrium faster towards a higher proportion of active form. Also the reduction of substrate (cysteine or for example, quinone) by selenolate will be faster.

Although the overall energy gain from the reduction of substrate cystine by NADPH is changed neither by the involvement of the swapping catalytic triad, nor that of selenocysteine, the flatter energy profile with its constantly downhill redox process within TrxR will make the process much faster, including the final electron transfer to the substrate. Of course, effects like protonation of the product by external water instead of internal reprotonation and conformational changes upon bindings and release of NADPH and NADP, respectively, could not be included. The energy gained by these processes not contained in our considerations may further drive the reaction equilibria.

Experimental Section

Theoretical methods: The program MOE©[47] was used for homology modelling of human thioredoxin reductase. The sequences of cytoplasmic human thioredoxin reductase (EC 1.8.1.9)[29] (Txn1, swiss-prot entry Q16881) and of mitochondrial human thioredoxin reductase (Txn2, swiss-prot entry Q9NNW7)[30–32] were taken from the swiss-prot database and were aligned with the one of rat thioredoxin reductase (pdb entry 1h6v)[6, 13, 28, 48] by using the blosum 62-matrix.[49, 50] For each protein, ten models were calculated by MOE and preoptimised by using the AMBER94 force field.[51] All ten models were checked with regard to stereochemical quality by using PROCHECK.[37] The best one was used for further refinement with the AMBER force field and subsequently, after manual addition of FAD and NADPH in positions taken from the rat template, the complete model was refined by using the TRIPOS force field[52] and Gasteiger charges,[53] which are implemented in the SYBYL molecular modelling package[54] running on Silicon Graphics workstations. The quality of the models was checked again with PROCHECK and also with PROSA II.[38] PROSA calculates the energy potentials for the atomic interactions of all amino acid residue pairs as a function of the distance between the corresponding atoms. The energies of all conformations that exist in an integrated data base with respect to the given sequence are calculated by using the potential of mean force, which has been derived by statistical analysis of a set of natively folded proteins. Negative energies of a PROSA II plot indicate that the modelled structures may represent a native fold, whereas sequences with positive energies would have to be critically inspected.

The X-ray structure of the reduced form of human thioredoxin was taken from the protein database (entry 1aiu).[27] The disulfide bond between Cys32′ and Cys35′ was closed manually by using SYBYL and a partial optimisation for the sequence Thr30′ to Met37′ was carried out.

The resulting structure was compared with the known X-ray structures of oxidised thioredoxins (PDB entries 1AUC[27] and 1ERU[55]), which were practically identical, except for small deviations in the loop forming the disulfide bridge between Cys32′ and Cys35′. The heat of formation of the oxidised fragment Cys-Gly-Pro-Cys calculated with the semiempirical PM5 method for the modelled structure is only 0.6 kcal mol^{-1} less stable than the one taken from the X-ray structure. However, the structure of the manually formed oxidised loop did provide a better fit to the active site of TrxR than those from the X-ray structures and was therefore used in further calculations. The modelled oxidised form of the ligand (Trx) was manually preoriented close to the active site of the model structures of human thioredoxin reductases. Two different orientations (180° rotation along a virtual axis parallel to the C-terminal tail of the enzyme) were tested for best docking arrangements, and, for these, molecular-dynamics simulations over 50 ps were performed with completely fixed thioredoxin reductase but free thioredoxin. During this first dynamics simulation, several constraints were applied in order to ensure the integrity of helical structural elements of the ligand. All backbone hydrogen bonds were kept by additional constraints within the helices. Furthermore, a low constraint was added between the sulfur atom of Cys32′ of thioredoxin and the selenium of Sec498 of the reductase. The resulting structures were optimised with the TRIPOS force field. Finally, to allow an optimal induced fit, a final run of dynamics simulations (100 ps) was performed (with subsequent optimisation) without any constraints but with a water box and the application of periodic boundary conditions by using MOE. The ab initio DFT calculations (B3LYP, lacv3p**) were performed with JAGUAR 4.1.[56] Full geometry optimisation was performed for all complexes investigated. Semiempirical PM5 calculations were performed by using the modelling program CaChe.[57]

Keywords: density functional calculations · enzyme catalysis · homolgy modeling · reductases · selenium

[1] M. Luthman, A. Holmgren, *Biochemistry* **1982**, *21*, 6628 – 6633.
[2] E. S. Arner, L. Zhong, A. Holmgren, *Methods Enzymol.* **1999**, *300*, 226 – 239.
[3] A. Holmgren, C. Lyckeborg, *Proc. Natl. Acad. Sci. USA* **1980**, *77*, 5149 – 5152.
[4] M. Björnstedt, S. Kumar, L. Björkhem, G. Spyrou, A. Holmgren, *Biomed. Environ. Sci.* **1997**, *10*, 271 – 279.
[5] M. Björnstedt, M. Hamberg, S. Kumar, J. Xue, A. Holmgren, *J. Biol. Chem.* **1995**, *270*, 11 761 – 11 764.
[6] L. Zhong, E. S. J. Arnér, J. Ljung, F. Åslund, A. Holmgren, *J. Biol. Chem.* **1998**, *273*, 8581 – 8591.
[7] S. N. Gorlatov, T. C. Stadtman, *Proc. Natl. Acad. Sci. USA* **1998**, *95*, 8520 – 8525.
[8] M. Berggren, A. Gallegos, J. Gasdaska, G. Powis, *Anticancer Res.* **1997**, *17*, 3377 – 3380.
[9] K. E. Hill, G. W. Mccollum, M. E. Boeglin, R. F. Burk, *Biochem. Biophys. Res. Commun.* **1997**, *234*, 293 – 295.
[10] V. N. Gladyshev, V. M. Factor, F. Housseau, D. L. Hatfield, *Biochem. Biophys. Res. Commun.* **1998**, *251*, 488 – 493.
[11] J. R. Gasdaska, J. W. Harney, P. Y. Gasdaska, G. Powis, M. J. Berry, *J. Biol. Chem.* **1999**, *274*, 25 379 – 25 385.
[12] N. Fujiwara, T. Fujii, J. Fujii, N. Taniguchi, *Biochem. J.* **1999**, *340*, 439 – 444.
[13] L. Zhong, A. Holmgren, *J. Biol. Chem.* **2000**, *275*, 18 121 – 18 128.
[14] S. Kumar, M. Björnstedt, A. Holmgren, *Eur. J. Biochem.* **1992**, *207*, 435 – 439.
[15] E. S. J. Arnér, A. Holmgren, *Eur. J. Biochem.* **2000**, *267*, 6102 6111.
[16] S. Gromer, L. D. Arscott, C. H. J. Williams, R. H. Schirmer, K. Becker, *J. Biol. Chem.* **1998**, *273*, 20 096 – 20 101.
[17] M. M. Maurice, H. Nakamura, S. Gringhuis, T. Okamoto, S. Yoshida, F. Kullmann, S. Lechner, E. A. Van Der Voort, A. Leow, J. Versendaal, U. Muller-Ladner, J. Yodoi, P. P. Tak, F. C. Breedveld, C. L. Verweij, *Arthritis Rheum.* **1999**, *42*, 2430 – 2439.
[18] V. N. Gladyshev, T. C. Stadtman, D. L. Hatfield, K. T. Jeang, *Proc. Natl. Acad. Sci. USA* **1999**, *96*, 835 – 839.
[19] G. W. Newman, M. K. Balcewicz-Sablinska, J. R. Guarnaccia, H. G. Remold, D. S. Silberstein, *J. Exp. Med.* **1994**, *180*, 359 – 363.
[20] H. Nakamura, S. De Rosa, M. Roederer, M. T. Anderson, J. G. Dubs, J. Yodoi, A. Holmgren, L. A. Herzenberg, *Int. Immunol.* **1996**, *8*, 603 – 611.
[21] K. Becker, S. Gromer, R. H. Schirmer, S. Müller, *Eur. J. Biochem.* **2000**, *267*, 6118 – 6125.
[22] M. P. Rigobello, G. Scutari, A. Folda, A. Bindoli, *Biochem. Pharmacol.* **2004**, *67*, 689 – 696.
[23] M. P. Rigobello, G. Scutari, R. Boscolo, A. Bindoli, *Br. J. Pharmacol.* **2002**, *136*, 1162 – 1168.

[24] C. H. Williams, L. D. Arscott, S. Müller, B. W. Lennon, M. L. Ludwig, P.-F. Wang, D. M. Veine, K. Becker, R. H. Schirmer, *Eur. J. Biochem.* **2000**, *267*, 6110 – 6117.
[25] L. Zhong, E. S. J. Arnér, A. Holmgren, *Proc. Natl. Acad. Sci. USA* **2000**, *97*, 5854 – 5859.
[26] T. W. Gilberger, R. D. Walter, S. Müller, *J. Biol. Chem.* **1997**, *272*, 29584 – 29589.
[27] J. F. Andersen, D. A. Sanders, J. R. Gasdaska, A. Weichsel, G. Powis, W. R. Montfort, *Biochemistry* **1997**, *36*, 13979 – 13988.
[28] E. S. Arnér, H. Sarioglu, F. Lottspeich, A. Holmgren, A. Bock, *J. Mol. Biol.* **1999**, *292*, 1003 – 1016.
[29] P. Y. Gasdaska, J. R. Gasdaska, S. Cochran, G. Powis, *FEBS Lett.* **1995**, *373*, 5 – 9.
[30] Q.-A. Sun, Y. Wu, F. Zappacosta, K.-T. Jeang, B. J. Lee, D. L. Hatfield, V. N. Gladyshev, *J. Biol. Chem.* **1999**, *274*, 24522 – 24530.
[31] P. Y. Gasdaska, M. M. Berggren, M. J. Berry, G. Powis, *FEBS Lett.* **1999**, *442*, 105 – 111.
[32] A. Miranda-Vizuete, A. E. Damdimopoulos, J. R. Pedrajas, J.-A. Gustafsson, G. Spyrou, *Eur. J. Biochem.* **1999**, *261*, 405 – 412.
[33] I. Chambers, J. Frampton, P. Goldfarb, N. Affara, W. Mcbain, P. R. Harrison, *EMBO J.* **1986**, *5*, 1221 – 1227.
[34] W. A. Günzler, G. J. Steffens, A. Grossmann, S. M. Kim, F. Otting, A. Wendel, L. Flohe, *Hoppe-Seyler's Z. Physiol. Chem.* **1984**, *365*, 195 – 212.
[35] F. Zinoni, A. Birkmann, T. C. Stadtman, A. Bock, *Proc. Natl. Acad. Sci. USA* **1986**, *83*, 4650 – 4654.
[36] T. Tamura, T. C. Stadtman, *Proc. Natl. Acad. Sci. USA* **1996**, *93*, 1006 – 1011.
[37] R. A. Laskowski, M. W. Macarthur, D. S. Moss, J. M. Thornton, *J. Appl. Crystallogr.* **1993**, *26*, 283 – 291.
[38] M. J. Sippl, *J. Comput.-Aided Mol. Des.* **1993**, *7*, 473 – 501.
[39] H. M. Berman, J. Westbrook, Z. Feng, G. Gilliland, T. N. Bhat, H. Weissig, I. N. Shindyalov, P. E. Bourne, *Nucleic Acids Res.* **2000**, *28*, 235 – 242.
[40] A. Barth, K. Frost, M. Wahab, W. Brandt, H. D. Schädler, R. Franke, *Drug Des. Discovery* **1994**, *12*, 89 – 111.
[41] A. Barth, M. Wahab, W. Brandt, K. Frost, *Drug Des. Discovery* **1993**, *10*, 297 – 317.
[42] D. M. Blow, J. J. Birktoft, B. S. Hartley, *Nature* **1969**, *221*, 337 – 340.
[43] R. M. Stroud, *Sci. Am.* **1974**, *231*, 74 – 78.
[44] R. E. Huber, R. S. Criddle, *Arch. Biochem. Biophys.* **1967**, *122*, 164 – 173.
[45] T. Y. Lin, T. S. Chen, *Biochemistry* **2004**, *43*, 945 – 952.
[46] S. Gromer, L. Johansson, H. Bauer, L. D. Arscott, S. Rauch, D. P. Ballou, C. H. J. Williams, R. H. Schirmer, E. S. Arner, *Proc. Natl. Acad. Sci. USA* **2003**, *100*, 12618 – 12623.
[47] "Molecular Operating Environment" (MOE) Program, Chemical Computing Group Inc., Montreal, Canada
[48] T. Sandalova, L. Zhong, Y. Lindqvist, A. Holmgren, G. Schneider, *Proc. Natl. Acad. Sci. USA* **2001**, *98*, 9533 – 9538.
[49] S. Henikoff, J. G. Henikoff, *Proc. Natl. Acad. Sci. USA* **1992**, *89*, 10915 – 10919.
[50] S. Henikoff, J. G. Henikoff, *Proteins* **1993**, *17*, 49 – 61.
[51] W. D. Cornell, P. Cieplak, C. I. Bayly, I. R. Gould, K. M. J. Merz, D. M. Ferguson, D. C. Spellmeyer, T. Fox, J. W. Caldwell, P. A. Kollman, *J. Am. Chem. Soc.* **1995**, *117*, 5179 – 5197.
[52] M. Clark, R. D. Cramer III, N. J. Van Opdenbosch, *J. Comput. Chem.* **1989**, *10*, 982 – 1012.
[53] J. Gasteiger, M. Marsili, *Tetrahedron* **1980**, *36*, 3219 – 3228.
[54] SYBYL©, Tripos Associates Inc., St. Louis, MO (USA).
[55] A. Weichsel, J. R. Gasdaska, G. Powis, W. R. Montfort, *Structure* **1996**, *4*, 735 – 751.
[56] Jaguar 4.1, Schrödinger Inc., Portland, OR (USA), **1991**–**2000**.
[57] CaChe WorkSystem Pro Version 6.1, Fujitsu Ltd. (Japan), **2000**–**2003**.

Received: August 2, 2004
Published online: January 13, 2005

